Human Reproduction, Vol.27, No.11 pp. 3259–3272, 2012
Advanced Access publication on August 28, 2012 doi:10.1093/humrep/des279

human reproduction

ORIGINAL ARTICLE *Reproductive biology*

Endometrial gene expression in the early luteal phase is impacted by mode of triggering final oocyte maturation in recFSH stimulated and GnRH antagonist co-treated IVF cycles

P. Humaidan[1,*], I. Van Vaerenbergh[2], C. Bourgain[2], B. Alsbjerg[3], C. Blockeel[4], F. Schuit[5], L. Van Lommel[5], P. Devroey[4], and H. Fatemi[4]

[1]The Fertility Clinic, Department D, Odense University Hospital, OHU, Entrance 55, Odense C 5000, Denmark [2]Reproductive Immunology and Implantation Unit, Dutch-speaking Free University of Brussels, Brussels, Belgium [3]The Fertility Clinic, Skive Regional Hospital, Skive, Denmark [4]Centre for Reproductive Medicine, Dutch-speaking Free University of Brussels, Brussels, Belgium [5]Gene Expression Unit, KU Leuven, Leuven, Belgium

*Correspondence address. Tel: +45-20-34-26-87; E-mail: peter.humaidan@ouh.regionsyddanmark.dk

Submitted on March 9, 2012; resubmitted on June 3, 2012; accepted on June 22, 2012

STUDY QUESTION: Do differences in endometrial gene expression exist after ovarian stimulation with four different regimens of triggering final oocyte maturation and luteal phase support in the same patient?

SUMMARY ANSWER: Significant differences in the expression of genes involved in receptivity and early implantation were seen between the four protocols.

WHAT IS KNOWN ALREADY: GnRH agonist triggering is an alternative to hCG triggering in GnRH antagonist co-treated cycles, resulting in an elimination of early ovarian hyperstimulation syndrome. Whereas previous studies have revealed a low ongoing clinical pregnancy rate after GnRH agonist trigger due to a high early pregnancy loss rate, despite supplementation with the standard luteal phase support, more recent studies, employing a 'modified' luteal phase support including a bolus of 1500 IU hCG on the day of oocyte aspiration, have reported ongoing pregnancy rates similar to those seen after hCG triggering.

STUDY DESIGN, SIZE DURATION: A prospective randomized study was performed in four oocyte donors recruited from an oocyte donation program during the period 2010–2011.

PARTICIPANTS, MATERIALS, SETTING, METHODS: Four oocyte donors in a university IVF center each prospectively underwent four consecutive stimulation protocols, with different modes of triggering final oocyte maturation and a different luteal phase support, followed by endometrial biopsy on Day 5 after oocyte retrieval. The following protocols were used: (A) 10 000 IU hCG and standard luteal phase support, (B) GnRH agonist (triptorelin 0.2 mg), followed by 1500 IU hCG 35 h after triggering final oocyte maturation, and standard luteal phase support, (C) GnRH agonist (triptorelin 0.2 mg) and standard luteal phase support and (D) GnRH agonist (triptorelin 0.2 mg) without luteal phase support. Microarray data analysis was performed with GeneSpring GX 11.5 (RMA algorithm). Pathway and network analysis was performed with the gene ontology software Ingenuity Pathways Analysis (Ingenuity® Systems, www.ingenuity.com, Redwood City, CA, USA). Samples were grouped and background intensity values were removed (cutoff at the lowest 20th percentile). A one-way ANOVA test ($P < 0.05$) was performed with Benjamini–Hochberg multiple testing correction.

MAIN RESULTS: Significant differences were seen in endometrial gene expression, related to the type of ovulation trigger and luteal phase support. However, the endometrial gene expression after the GnRH agonist trigger and a modified luteal phase support (B) was similar to the pattern seen after the hCG trigger (A).

LIMITATIONS, REASONS FOR CAUTION: The study was performed in four oocyte donors only; however, it is a strength of the study that the same donor underwent four consecutive stimulation protocols within 1 year to avoid inter-individual variations.

WIDER IMPLICATIONS OF THE FINDINGS: These endometrial gene-expression findings support the clinical reports of a non-significant difference in live birth rates between the GnRH agonist trigger and the hCG trigger, when the GnRH agonist trigger is followed by a bolus of 1500 IU hCG at 35 h post trigger in addition to the standard luteal phase support.

STUDY FUNDING/ COMPETING INTERESTS: This study was supported by an un-restricted research grant by MSD Belgium.

TRIAL REGISTRATION NUMBER: EudraCT number 2009-009429-26, protocol number 997 (P06034).

Key words: endometrium / gene expression / GnRH antagonist / GnRH agonist trigger / hCG

Introduction

In assisted reproductive technology (ART), a bolus of hCG, 5000–10 000 IU, is administered either subcutaneously or intramuscularly to mimic the mid-cycle surge of LH. Due to their structural similarities, hCG and LH bind to and activate the same receptor, the LH/hCG receptor (Kessler *et al.*, 1979), and it is assumed that exogenous hCG promotes the same biological processes as the natural mid-cycle surge of LH. There are, however, significant molecular and structural differences between LH and hCG. Importantly, the half-life of hCG is longer (days) than that of LH (hours), due to an increased content of oligosaccharides (Damewood *et al.*, 1989). Moreover, in contrast to a bolus of hCG, in the natural cycle, both LH and FSH are secreted during the mid-cycle surge of gonadotrophins. The FSH surge is known to promote nuclear maturation, i.e. the resumption of meiosis, as well as LH receptor formation in the luteinizing granulosa cells, securing the function of the corpus luteum during the subsequent luteal phase (Strickland and Beers, 1976; Eppig, 1979; Zelinski-Wooten *et al.*, 1995; Yding *et al.*, 1999; Yding, 2002).

A bolus of GnRH agonist was previously shown to effectively stimulate ovulation and final oocyte maturation, inducing an initial secretion of LH and FSH (flare-up) from the pituitary, similar to that seen during the natural mid-cycle surge of gonadotrophins, prior to down-regulation of the GnRH receptor (Gonen *et al.*, 1990; Itskovitz *et al.*, 1991). However, with the introduction of GnRH agonist for pituitary down-regulation prior to IVF/ICSI treatment (Porter *et al.*, 1984), this concept was not applicable any longer, as the simultaneous use of GnRH agonist for down-regulation and triggering of final oocyte maturation is not possible.

Recently, when the GnRH antagonist was introduced, it became feasible again to trigger ovulation with a bolus of a GnRH agonist, as a bolus of GnRH agonist will displace the GnRH antagonist from the GnRH receptor, eliciting a surge of LH and FSH (Humaidan *et al.*, 2005, 2006, 2010; Humaidan, 2009; Engmann *et al.*, 2008).

The first RCT to re-introduce GnRH agonist triggering in patients co-treated with a GnRH antagonist had to be discontinued due to an extremely high early pregnancy loss rate (79%), despite supplementation with a standard luteal phase support including vaginal progesterone as well as estradiol (Humaidan *et al.*, 2005). Following this trial, a number of studies were performed, showing an optimal intra-follicular environment after GnRH agonist trigger (Andersen *et al.*, 2006), a live birth rate after frozen embryo replacement comparable with that seen after the hCG trigger (Griesinger *et al.*, 2007) and intra-follicular amphiregulin levels after the GnRH agonist trigger closer to those seen after the natural mid-cycle surge of gonadotrophins than those seen after the hCG trigger (Humaidan *et al.*, 2011). Furthermore, several studies reported the retrieval of more MII oocytes after the GnRH agonist trigger when compared with the hCG trigger (Imoedemhe *et al.*, 1991; Humaidan *et al.*, 2005, 2010, 2011; Oktay *et al.*, 2010). However, on the basis of the abovementioned studies, it was hypothesized that the GnRH agonist trigger induces a further disruption of the luteal phase seen after controlled ovarian stimulation, due to a significant reduction in circulating endogenous LH during the early-mid luteal phase when compared with the natural cycle (Humaidan, 2009). In contrast, after the hCG trigger, this LH deficiency is covered by the prolonged LH-like activity of hCG (Weissman *et al.*, 1996; Fauser *et al.*, 2002).

To confirm the LH deficiency theory after the GnRH agonist trigger, a number of trials were conducted during which the luteal phase support was modified, as patients, in addition to a standard luteal phase support, were supplemented with a small bolus of LH-like activity in the form of 1500 IU hCG on the day of oocyte retrieval (Humaidan *et al.*, 2006, 2010; Humaidan, 2009). The results of these studies seemed to confirm the LH deficiency theory, as the luteal phase after GnRH agonist triggering was normalized in these patients not only in terms of serum progesterone levels, but also in terms of the reproductive outcome, as clinical pregnancy rates were similar to those seen after the hCG trigger (Humaidan *et al.*, 2006, 2010; Humaidan, 2009).

The objective of the present study was to mimic, in an oocyte donor model, the set-up of the clinical trials previously performed with the GnRH agonist trigger to analyze the impact on endometrial gene expression. To avoid any inter-individual variation in gene expression, each donor performed four consecutive oocyte donation cycles within 1 year.

Materials and Methods

Patient population

Four oocyte donors were included in the trial performed during the period 2010–2011. Each donor performed four oocyte donation cycles, randomized to different models of final oocyte maturation and luteal phase support; thus, a total of 16 oocyte donation cycles performed in four oocyte donors were analyzed.

The inclusion criteria were: the presence of a minimum of five antral follicles in each ovary, normal chromosomal analysis, normal serological findings within 3 months prior to stimulation, normal vaginal ultrasound (US) and no presence of any intrauterine contraceptive device.

The exclusion criteria were: the presence of polycystic ovarian syndrome diagnosed according to the revised Rotterdam criteria (Rotterdam ESHRE/ASRM–Sponsored PCOS Consensus Workshop Group 2004), presence of endometriosis AFS classification stage >2, age ≥36 years,

US verified hydrosalpinges, presence of any intrauterine contraceptive device and/or OCP usage for the past 6 months prior to the initiation of stimulation.

The research project was approved by the local Institutional Review Board and registered in the European Community Clinical Trial System (EudraCT) number 2009-009429-26, protocol number 997 (P06034).

Ovarian stimulation

After a vaginal US examination and the confirmation of baseline FSH, LH and estradiol, stimulation commenced in the afternoon of Day 2 of the cycle with 200 IU rec-FSH (Puregon®, MSD, Oss, the Netherlands). The FSH dose remained fixed until Day 5 of the cycle. Thereafter, the FSH dose was adjusted according to the ovarian response. To inhibit a premature LH surge, daily GnRH antagonist co-treatment (Orgalutran® 0.25 mg, MSD) was implemented from the morning of Day 5 of stimulation. Final oocyte maturation was induced as soon as $\geq$3 follicles of $\geq$17 mm were present. Randomization to one of the four protocols, through a computer generated list, took place on the day of triggering of final oocyte maturation. Once patients had been allocated to one of the possible protocols, this protocol was automatically deleted from the computer generated list. Oocyte retrieval was carried out 34 h later. In addition, the gynecologist in charge of the oocyte retrieval and the scientist responsible for the gene expression analyses of endometrial biopsies were blinded to the treatment allocation.

Final oocyte maturation

The same donor underwent four stimulation protocols with different modes of final oocyte maturation and luteal phase support: (A) 10 000 IU hCG and standard luteal phase support, (B) triptorelin 0.2 mg, followed by 1500 IU hCG 35 h after triggering of final oocyte maturation and standard luteal phase support, (C) triptorelin 0.2 mg with standard luteal phase support and (D) triptorelin 0.2 mg without luteal phase support.

Luteal phase support

The standard luteal phase support consisted of vaginal administration of 600 mg natural micronized progesterone in three separate doses (Utrogestan®, Besins-Iscovesco, Paris, France, 100 mg 3 × 2/day) with the addition of estradiol-valerate (Progynova®, Schering N.V, Diegem, Belgium) 4 mg daily per o.s., starting 1 day after oocyte retrieval and continuing until the day of endometrial sampling, day ovum pick up + 5.

US assessment

US was performed on Day 6 of stimulation and thereafter as necessary in order to ensure that final oocyte maturation was triggered on the day when the patient had $\geq$3 follicles of $\geq$17 mm.

Endometrial sampling and RNA isolation

Endometrial biopsies were taken with a pipelle cannula (Pipelle de Cornier®, Prodimed, Neuilly-en-Thelle, France) under sterile conditions on the 5th day after the oocyte retrieval. Biopsies were snap-frozen in liquid nitrogen under sterile conditions for RNA isolation. To avoid a short-time bias in endometrial gene expression due to the biopsy, donors underwent stimulation and biopsy with an interval of 3 months.

RNA extraction was performed using the RNeasy Mini kit (Qiagen, Valencia, CA, USA). Total RNA concentration was measured with the NanoDrop ND-1000 spectrophotometer (NanoDrop Technologies, Wilmington, DE, USA) and integrity of the RNA samples was controlled using the Agilent 2100 Bioanalyzer with the RNA 6000 Nano Kit (Agilent Technologies Inc., Palo Alto, CA, USA).

Microarrays and data analysis

In total, 16 samples were analyzed for their gene expression with microarrays. Therefore, 500 ng of the total RNA was reverse-transcribed with the IVT express kit (Affymetrix, Santa Clara, CA, USA) with oligo-dT primers containing a T7 RNA polymerase promotor site. Then, cDNA was *in vitro* transcribed and labeled with biotin followed by the fragmentation of the biotinylated cRNA. Next, the quality of this cRNA was assessed with the Agilent 2100 Bioanalyzer and NanoDrop. Quality control of prepared cRNA samples was based on (i) a yield of $>$15 μg and (ii) a Bioanalyzer microchannel electrophoresis elution profile that was typical for the chosen tissue and reproducible for the replicate samples (Van Lommel *et al.*, 2006). The fragmented cRNA was hybridized overnight to the Affymetrix Human Genome (HG) U133 Plus 2.0 Array (Affymetrix). This array contains more than 54 000 probe sets for the whole HG. Subsequently, the arrays were washed and stained according to the protocol (Affymetrix Expression Analyses Technical Manual 702646Rev1) and scanned on an Affymetrix 3000 GeneScanner.

Data analysis was performed with GeneSpring GX 11.5 (RMA algorithm; Van Vaerenbergh *et al.*, 2009). Pathway and network analysis was performed with the gene ontology software Ingenuity Pathways Analysis (Ingenuity® Systems, www.ingenuity.com, Redwood City, CA, USA; Van Vaerenbergh *et al.*, 2009).

Validation of microarrays: quantitative PCR

To verify the results obtained from the microarrays on the RNA level, three selected genes were validated with a more quantitative real-time PCR technique. Genes were selected based on evidence from the literature related to the endometrial expression of genes during the peri-implantation period and the uterine receptivity (Lindhard *et al.*, 2002; Pilka *et al.*, 2003; Ledee-Bataille *et al.*, 2004, 2005) and based on their high fold change and/or their appearance in the involved pathways.

A two-step real-time PCR was performed. First, a reverse-transcription reaction from total RNA was achieved with the High-Capacity cDNA Archive kit (Applied Biosystems, Foster City, CA, USA) following the manufacturer's protocol. The quantitative real-time PCR was performed with the TaqMan Gene Expression Assays (Applied Biosystems). Glyceraldehyde-3-phosphate dehydrogenase (GAPDH) was chosen as the control housekeeping gene using the TaqMan Endogenous Control Assay (Applied Biosystems). Both assays are cDNA specific, since the probes span an exon junction. All real-time PCR assays were run using the TaqMan Gene Expression Master Mix (Applied Biosystems) on the 7900 HT Fast System (Applied Biosystems). Thermal cycling parameters were set as follows: 2 min at 50°C, 10 min at 95°C, followed by 40 cycles of denaturation, annealing and extension (15 s at 95°C and 1 min at 60°C, respectively). All samples were analyzed in triplicate. The relative quantification was performed by the standard curve method. For each sample, the amount of target gene and endogenous control (GAPDH) was determined from their respective standard curves. First, the target gene amount was divided by the endogenous control amount to obtain a normalized value. In a second step, the samples were normalized again to the sample with the lowest normalized expression, the calibrator sample or 1× sample. Therefore, each of the normalized values was divided by the calibrator-normalized value to generate the relative expression levels.

Data analysis and statistical methods

The microarray data analysis was performed with GeneSpring GX 11.5 (RMA algorithm). Pathway and network analysis was performed with the gene ontology software Ingenuity Pathways Analysis (Ingenuity® Systems, www.ingenuity.com). Samples were grouped and background intensity

values were removed (cutoff lowest 20 percentile). A one-way ANOVA test ($P < 0.05$) was performed with the Benjamini–Hochberg multiple testing correction for the false discovery rate at 0.05.

Results

Differentially expressed genes

The four study groups were compared with each other, with Group A as the control group.

From quality-control steps (with PCA and hierarchical clustering), it was shown that one sample was considered as an outlier. Indeed, when correlating this with the available histological dating results, we found that the dating for this biopsy sample was not possible due to the fact that this sample contained isthmus material. This sample, therefore, was excluded from the following analysis.

Thus, a total of 15 samples were used for analysis. Samples were grouped and background intensity values were removed (cutoff lowest 20 percentile). A one-way ANOVA test ($P < 0.05$) was performed with the Benjamini–Hochberg multiple testing correction. There were 2631 entities or probe sets which had a fold change cutoff of 2.0 in at least one condition pair, when comparing Group A with Group B, or A with C, A with D, B with C, B with D and C with D (Supplementary data, Table SI).

From this gene list, the groups were compared separately (Supplementary data, Tables SII–SVII). The number of significantly differentially expressed probe sets ($P < 0.05$; FC ≥ 2.0) is shown in Table I. This difference in gene expression can be visualized by a profile plot (Fig. 1). A profile plot is a graphical data analysis technique to examine the relative behavior of all variables in a multivariate data set. This data analysis in Fig. 1 shows all the significantly differentially expressed probe sets or genes, represented by lines. Each line represents a gene and each line is colored by its expression in Group A. The expression of each gene can therefore be followed in the four treatment groups. This analysis shows a large difference between Group D and the other groups and a small difference in gene expression between Groups A and B. Groups A and B are similar in gene expression, while Groups C and D show more differences in gene expression, when compared with each other and also compared with Groups A and B. In Group D, some genes show a very extreme up- or down-regulation. These genes are INHBA (inhibin-βa), MMP1 and MMP3 (matrix metalloproteinases 1 and 3), LEFTY2 [endometrial bleeding associated factor (left-right determination, factor A) transforming growth factor beta (TGF-β) superfamily], which were up-regulated in Group D, and CXCL13 [chemokine (C-X-C motif) ligand 13], MMP26 and SCGB1D2 (secretoglobin family 1D member 2 or lipophilin B), which were down-regulated in Group D.

When comparing Groups B and C, a total of 785 probe sets were significantly differently expressed (Table I and Supplementary data, Table SV). From these genes, the top genes that were found to be highly up- or down-regulated in Group B included growth factors like TGFβ2, metalloproteinases like MMP26 and CYP3A5 (cytochrome P450), known for its role in steroidogenesis. Moreover, XDH (xanthine dehydrogenase) was highly up-regulated in Group B. This gene was previously found in a molecular network together with COX-2 in endometrial biopsies taken on the day of oocyte retrieval in stimulated IVF cycles (Van Vaerenbergh et al., 2011).

Table I Significantly differentially expressed entities or probe sets between groups.

Condition pairs	Number of probe sets
A–B	2 (up in A: 1; down in A: 1)
A–C	900 (up in A: 590; down in A: 310)
A–D	2595 (up in A: 1347; down in A: 1248)
B–C	785 (up in B: 495; down in B: 290)
B–D	2407 (up in B: 1217; down in B: 1190)
C–D	1228 (up in C: 437; down in C: 791)

Pathways, networks and functions

From the gene list of 2631 probe sets, the involved pathways and networks (Tables II and III) were investigated. From this data set, 25 networks could be formed. The most significant functions and diseases associated with these data are cancer, cellular movement, reproductive system disease, cell-to-cell signaling, cellular development, growth and proliferation. Furthermore, the analysis demonstrated a large number of pathways involved in, for example, natural killer cell signaling, arachidonic acid metabolism, phospholipase C signaling, TGF-β signaling, integrin signaling (Fig. 2), metabolism of xenobiotics by cytochrome P450, p53 signaling and Wnt/β-catenin signaling.

Quantitative PCR

Three genes were selected for further validation with quantitative real-time PCR, as described in the 'Materials and methods' section: MMP26 (matrix metallopeptidase 26), ITGB6 (integrin, β6) and IL12RB1 (interleukin 12 receptor, β1). The data showed a highly significant difference between Groups A and D in the expression of ITGB6 (unpaired *t*-test; $P = 0.0018$). The difference for IL12RB1 and MMP26 expression was not significant ($P > 0.05$), although a trend was noticeable.

Discussion

This study performed in an oocyte donor model revealed significant differences in early luteal phase endometrial gene expression according to the mode of triggering final oocyte maturation and the use or not of the luteal phase support. Four donors each underwent four consecutive oocyte donation cycles, using different protocols (A–D) to mimic the conditions previously described in randomized controlled trials (Beckers et al., 2003; Humaidan et al., 2005, 2010; Kolibianakis et al., 2005). Whereas Groups A and B were similar in gene expression, differences were seen not only between Group A or B and Group C or D, but also between Groups C and D. Importantly, the genes involved are well-known for their role in implantation.

The luteal phase of all stimulated IVF cycles is abnormal (Edwards et al., 1984) regardless of the type of GnRH analog used for co-treatment when compared with only 8% of natural cycles (Rosenberg et al., 1980). The most plausible reason for the disrupted luteal phase seen after ovarian stimulation seems to be the supra-physiological luteal steroid level, mainly progesterone, induced by

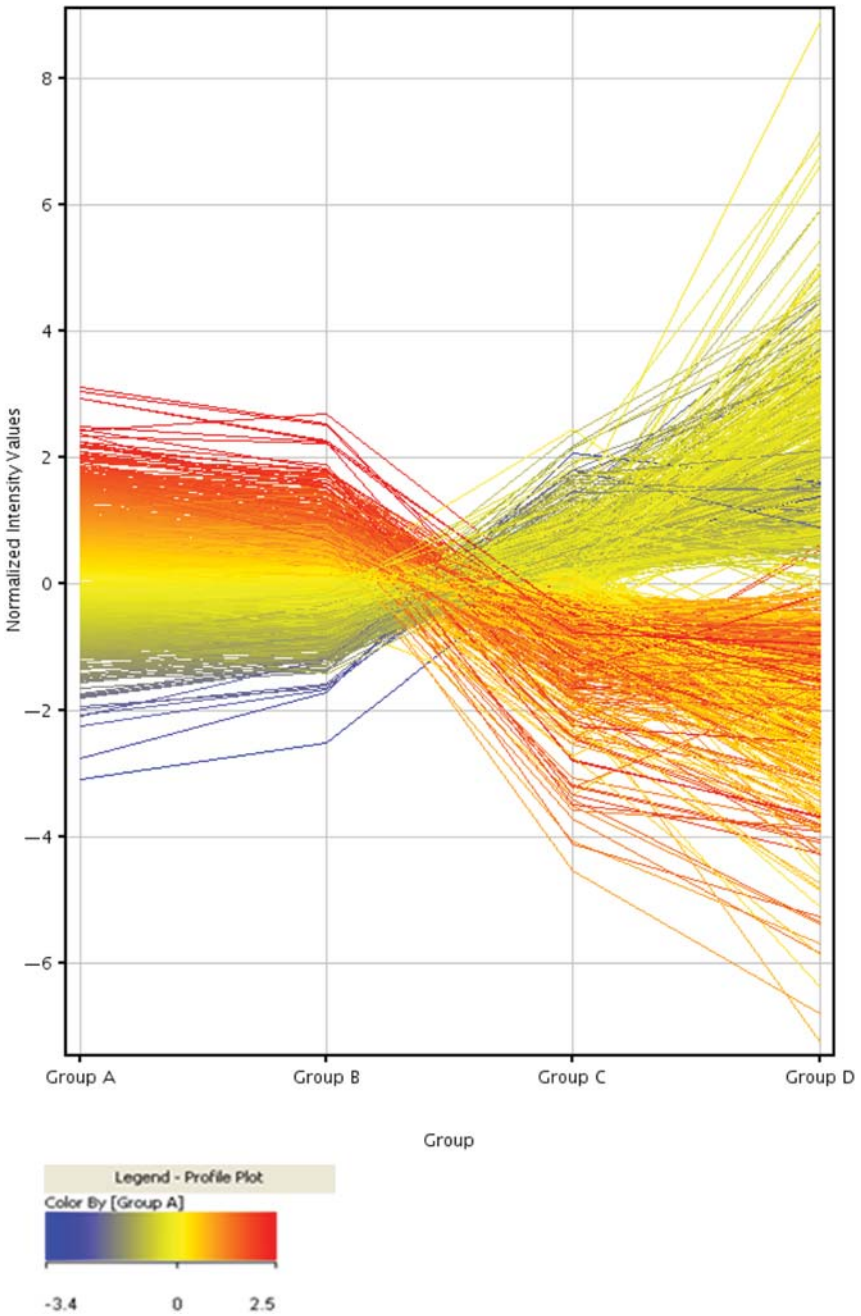

Figure 1 Profile plot displaying 2631 probe sets significantly differently expressed in at least one condition pair with Group A as the control condition. Probe sets are Colored by Group A. Up-regulated probe sets in red and down-regulated probe sets in blue.

the ovarian stimulation with exogenous gonadotrophins, exerting a negative feedback on the hypothalamic-pituitary axis level, leading to a reduction in LH secretion by the pituitary (Tavaniotou *et al.*, 2001; Tavaniotou and Devroey, 2006; Fatemi *et al.*, 2008). Importantly, GnRH agonist triggering *per se* induces a significant reduction in circulating endogenous LH in the early-to-mid-luteal phase due to differences in the profile and duration of the LH surge when compared with the natural mid-cycle surge of gonadotrophins (Hoff *et al.*, 1983; Gonen *et al.*, 1990; Itskovitz *et al.*, 1991) and it has previously been demonstrated that withdrawal of or a reduction in circulating LH during the luteal phase leads to luteolysis and implantation failure (Duffy *et al.*, 1999).

In contrast, when a large bolus of hCG (5000–10 000 IU) is used for the induction of ovulation, this ovulatory bolus of LH activity will support the corpora lutea for 7–10 days due to the long half-life of hCG (Eppig, 1979; Mannaerts *et al.*, 1998). From then on, the corpora lutea will be dependent on the endogenous LH secretion by the pituitary or by the gradually increasing hCG production from an implanting embryo, which actively secretes hCG, detectable in the maternal serum as early as from the 8th day after ovulation

Table II From the gene list of 2631 probe sets, the involved pathways were investigated with Ingenuity.

	Ingenuity canonical pathways	−log(*P*-value)	Molecules
1	Leukocyte extravasation signaling	5.78	RAP1B, RAC2, MMP7, MMP3, MMP14, JAM2, ABL1, CTNNA2, MMP26, MMP8, CYBA, MMP11, RASSF5, ACTG2, CTNNB1, MMP12, PRKD3, MMP1, ITK, PRKCA, ITGA4, TIMP2, MMP19, TIMP3, CLDN10, PRKCQ, CXCR4, MAPK8, MMP10, MMP2, ITGAL, SELPLG, ARHGAP5, MMP27, WIPF1, ITGAM, ARHGAP9, CLDN8, PIK3CD, CTTN, MSN
2	Valine, leucine and isoleucine degradation	4.72	ECHS1, ACAT2, ABAT, ACAA2, BCKDHB, BCAT1, PCCA, BCAT2, HIBADH, ALDH3A2, MCEE, ACAT1, DBT, OXCT1, MCCC1, EHHADH, ALDH6A1, HADH
3	Fatty acid metabolism	3.83	ACSL3, CPT1A, ACAT2, ECHS1, SLC27A2, CYP3A5, ACAA2, ADH5, CYP3A4, CYP2C18, DHRS9, ECI2, CYP4B1, ALDH3A2, ACAT1, CYP4X1, ACSL4, PECR, CYP2J2, EHHADH, HADH, CYP51A1, DHRS4
4	Propanoate metabolism	3.43	AASDH, ACSL3, ECHS1, ACAT2, ABAT, SUCLA2, PCCA, SRD5A3, DHCR24, ALDH3A2, ACSS2, MCEE, ACAT1, EHHADH, ALDH6A1
5	Human embryonic stem cell pluripotency	3.41	FZD10, TCF4, TGFBR1, FGF2, BMP2, BMPR2, LEFTY2, NOG, TCF7, WNT7A, TGFB1, MRAS, PDGFRA, TGFB2, AKT3, CTNNB1, FZD2, GNAS, S1PR2, TCF3, FZD4, FZD6, PIK3CD, PDGFD, WNT5A, POU5F1
6	Factors promoting cardiogenesis in vertebrates	3.29	FZD10, TCF4, PRKCQ, TGFBR1, SMAD9, BMP2, ACVR1, BMPR2, TCF3, TCF7, NOG, CCNE1, FZD4, TGFB1, TGFB2, FZD6, CTNNB1, PRKD3, FZD2, PRKCA
7	Bladder cancer signaling	2.93	CDKN2A, MMP7, MMP3, THBS1, FGF2, MMP14, ABL1, MMP10, MMP2, MMP27, MMP8, MMP26, MRAS, MMP11, RPS6KA5, ERBB2, MMP12, MMP1, MMP19
8	Glycosphingolipid biosynthesis–neolactoseries	2.79	ST8SIA4, GCNT3, FUT2, B3GNT2, GCNT2, ST8SIA2, B3GNT5, ST3GAL5
9	Colorectal cancer metastasis signaling	2.77	FZD10, MMP7, TCF4, TGFBR1, MMP3, MMP14, TCF7, WNT7A, GNG11, RHOB, TGFB1, MMP8, MMP26, TGFB2, MRAS, AKT3, MMP11, TLR3, CTNNB1, MMP12, FZD2, GNG4, MMP1, MMP19, GNAS, MAPK8, MMP10, MMP2, RHOJ, IFNGR1, TCF3, MMP27, FZD4, TLR5, PRKAG2, FZD6, PIK3CD, GNG2, WNT5A
10	T helper cell differentiation	2.77	TGFBR1, IL12RB1, IFNGR2, HLA-DRB1, RORC, HLA-DMB, IFNGR1, STAT4, TGFB1, FCER1G, IL10RA, HLA-DOB, GATA3, TNFRSF1B, TNFRSF11B
11	Aryl hydrocarbon receptor signaling	2.69	CDKN2A, IL1A, CHEK1, TGM2, TGFB1, ALDH3A2, TGFB2, ALDH6A1, GSTK1, MGST1, NQO1, ALDH8A1, MAPK8, CDK6, GSTO1, ALDH3B2, CCNE1, MGST2, ALDH1L2, NFIA, IL1B, NFIB, NCOR2, NRIP1, MCM7
12	Xenobiotic metabolism signaling	2.62	MAP2K6, CHST4, IL1A, CAMK1D, SULT1C2, HS3ST3A1, CHST15, CYP3A5, HS6ST1, CAMK2D, ALDH3A2, MRAS, CHST11, SMOX, HS3ST1, SULT1E1, PRKD3, ALDH6A1, GSTK1, PRKCA, MGST1, PRKCQ, MAP3K6, NQO1, MAPK8, ALDH8A1, GSTO1, ESD, ALDH3B2, MGST2, ALDH1L2, CYP3A4, PPP2R3A, IL1B, PIK3CD, NCOR2, NRIP1, ABCC3, PPP2R1B, MAOA
13	Natural killer cell signaling	2.61	CD247, RAC2, PRKCQ, PAK6, TYROBP, KLRD1, RAC3, KIR2DL4/LOC100287534, CD300A, KLRK1, FCER1G, MRAS, AKT3, KLRC3, PIK3CD, SH2D1B, PRKD3, LCP2, PRKCA, KLRC1
14	Agrin interactions at neuromuscular junction	2.55	RAC2, GABPB1, PAK6, ITGA2, LAMA2, MAPK8, RAC3, ITGAL, ITGB3, ERBB4, MRAS, ACTG2, ERBB2, CTTN, ITGA4
15	Glycine, serine and threonine metabolism	2.55	PSAT1, PISD, AMT, PLCB4, PLCE1, GCSH, DBT, PLCB1, SHMT1, SMOX, GOT1, GCAT, ALAS2, CTH, MAOA
16	LPS/IL-1 mediated inhibition of RXR function	2.55	CHST4, SLC27A2, SULT1C2, CHST15, HS3ST3A1, CYP3A5, ABCB9, HS6ST1, SCARB1, ALDH3A2, ACSL4, CHST11, SMOX, HS3ST1, SULT1E1, TNFRSF1B, ALDH6A1, GSTK1, TNFRSF11B, MGST1, ACSL3, CPT1A, ALDH8A1, MAPK8, GSTO1, ALDH3B2, MGST2, ALDH1L2, CYP3A4, IL1B, ABCC3, MAOA
17	Arachidonic acid metabolism	2.51	PLA2G12A, PTGS1, GGT6, PTGDS, CBR3, CYP3A5, PLA2G4A, CYP3A4, CYP2C18, MGST2, CYP4B1, GPX2, CYP4X1, PLA2G4F, CYP2J2, TBXAS1, CYP51A1, DHRS4, GSTK1
18	Molecular mechanisms of cancer	2.49	CDKN2A, RAP2B, RAC2, TGFBR1, CTNNA2, CAMK2D, RHOB, TGFB1, MRAS, PLCB1, HIPK2, BRCA1, FZD2, PRKD3, PRKCQ, SMAD9, CDK6, RHOJ, TCF3, RAC3, DAXX, FZD6, PIK3CD, MAP2K6, RAP1B, FZD10, TCF4, RALA, BMP2, ABL1, BMPR2, CDKN2B, CHEK1, TGFB2, AKT3, BID, ARHGEF2, CTNNB1, PRKCA, PMAIP1, GNAS, PAK6, GNA12, MAPK8, PLCB4, CCNE1, FZD4, RASGRP1, PRKAG2, BCL2L11, WNT5A
19	Methionine metabolism	2.41	TGM2, DNMT3A, MTR, AHCYL2, CTH, BHMT2, AMD1, AHCY

Continued

Table II *Continued*

	Ingenuity canonical pathways	−log(*P*-value)	Molecules
20	Phospholipase C signaling	2.41	RAP1B, CD247, NAPEPLD, RALA, RPS6KA3, HDAC9, TGM2, PLCE1, GNG11, AHNAK, RHOB, MRAS, PLCB1, ARHGEF2, PLA2G4F, MARCKS, GNG4, PRKD3, ITK, ITGA4, PRKCA, GNAS, PRKCQ, PLA2G12A, HDAC2, ITGA2, MEF2A, PPP1R14A, RHOJ, PLD1, PLA2G4A, MYL12A, PLCB4, FCER1G, GNG2, LCP2
21	TGF-β signaling	2.32	MAP2K6, RUNX3, TGFBR1, SMAD9, BMP2, ACVR1, MAPK8, BMPR2, TGIF1, INHBA, SMURF1, RUNX2, TGFB1, MRAS, TGFB2, SMURF2, VDR
22	Integrin signaling	2.29	RAP1B, RAP2B, RAC2, RALA, ABL1, RHOB, MRAS, AKT3, ACTG2, ITGB5, ITGA4, CAPN6, PAK6, ASAP1, ITGA2, MAPK8, RHOJ, RAC3, ITGAL, ITGB3, ARHGAP5, MYL12A, WIPF1, ITGAM, TSPAN1, ZYX, PIK3CD, ITGB6, TSPAN6, CTTN, NEDD9, ITGAX
23	Chondroitin sulfate biosynthesis	2.26	HS6ST1, CSGALNACT2, CHST4, CHSY1, CHST11, SULT1C2, HS3ST1, SULT1E1, HS3ST3A1, CHST15, DSE
24	Metabolism of xenobiotics by cytochrome P450	2.22	MGST1, CYP3A5, GSTO1, ADH5, ALDH3B2, CYP2C18, MGST2, DHRS9, CYP3A4, CYP4B1, CYP4X1, CYP2J2, PECR, CYP51A1, DHRS4, GSTK1
25	VDR/RXR activation	2.22	IGFBP6, CYP24A1, PRKCQ, IGFBP5, HES1, CAMP, RUNX2, TGFB2, IGFBP3, NCOR2, IGFBP1, VDR, CST6, PRKD3, HSD17B2, PRKCA
26	p53 signaling	2.15	CDKN2A, PLAGL1, PMAIP1, JMY, THBS1, TNFRSF10B, MAPK8, TP53BP2, CHEK1, SERPINE2, TP53I3, KAT2B, AKT3, PIK3CD, BRCA1, HIPK2, CTNNB1, DRAM1
27	Virus entry via endocytic pathways	2.06	RAC2, PRKCQ, ITGA2, ABL1, ITGAL, RAC3, ITGB3, FOLR1, MRAS, PIK3CD, ACTG2, ITGB6, CXADR, PRKD3, ITGB5, PRKCA, ITGA4
28	Tumoricidal function of hepatic natural killer cells	2.03	ENDOG, PRF1, SERPINB9, SRGN, BID, ITGAL, GZMB
29	HER-2 signaling in breast cancer	2.01	PRKCQ, CDK6, MMP2, PARD6G, ITGB3, CCNE1, TSC2, MRAS, AKT3, PIK3CD, ERBB2, ITGB6, PRKD3, ITGB5, PRKCA
30	Wnt/β-catenin signaling	1.99	CDKN2A, FZD10, TCF4, MMP7, TGFBR1, SFRP2, TLE1, TCF7, SOX17, CSNK1E, SOX9, WNT7A, TGFB1, TGFB2, AKT3, CTNNB1, FZD2, SOX4, ACVR1, TCF3, FZD4, PPP2R3A, FZD6, TLE3, PPP2R1B, WNT5A, POU5F1
31	Butanoate metabolism	1.94	BDH1, ECHS1, ACAT2, ABAT, ALDH3A2, GAD1, ACAT1, OXCT1, DBT, DCXR, EHHADH, HADH
32	G protein signaling mediated by tubby	1.91	PLCB4, GNG11, GNAS, MRAS, ABL1, PLCB1, GNG2, GNG4
33	Glioma invasiveness signaling	1.88	TIMP3, F2R, RHOB, MRAS, PLAUR, RHOJ, MMP2, PIK3CD, PLAU, ITGB5, TIMP2, ITGB3
34	CCR5 signaling in macrophages	1.86	CD247, GNAS, PRKCQ, MAPK8, CCL3, GNG11, CCL4, MRAS, FCER1G, GNG2, PRKD3, GNG4, PRKCA
35	Pantothenate and CoA biosynthesis	1.86	PANK1, ENPP3, CRMP1, BCAT1, BCAT2, DPYSL3
36	Crosstalk between dendritic cells and natural killer cells	1.86	KLRD1, TYROBP, CD69, TNFSF10, HLA-DRB1, KIR2DL4/LOC100287534, IL2RB, ITGAL, PRF1, CAMK2D, FSCN1, KLRK1, ACTG2, TLR3, TNFRSF1B, PVRL2
37	Synthesis and degradation of ketone bodies	1.83	BDH1, ACAT2, ACAT1, OXCT1
38	Role of osteoblasts, osteoclasts and chondrocytes in rheumatoid arthritis	1.82	MAP2K6, FZD10, TCF4, IL1A, SFRP2, MMP3, BMP2, MMP14, BMPR2, TCF7, SMURF1, WNT7A, TGFB1, RUNX2, MMP8, AKT3, TRAF5, CTNNB1, TNFRSF1B, FZD2, MMP1, TNFRSF11B, ACP5, SMAD9, ITGA2, MAPK8, TCF3, ITGB3, FZD4, FZD6, IL1B, PIK3CD, WNT5A
39	Cysteine metabolism	1.80	HS6ST1, CHST4, CHST11, GOT1, SULT1C2, HS3ST1, SULT1E1, CTH, HS3ST3A1, CHST15
40	Glycosphingolipid biosynthesis−globoseries	1.76	ST3GAL2, ST8SIA4, FUT2, GM2A, ST8SIA2, B3GALNT1
41	Inhibition of angiogenesis by TSP1	1.75	TGFBR1, THBS1, SDC2, TGFB1, KDR, MAPK8, CD36, AKT3
42	Keratan sulfate biosynthesis	1.74	HS6ST1, ST3GAL2, CHST4, B3GNT2, CHST11, SULT1C2, HS3ST1, SULT1E1, HS3ST3A1, CHST15
43	Glutathione metabolism	1.74	GSR, MGST1, MGST2, GPX2, GGT6, GGCT, GLRX, GSTO1, GSTK1, IDH1
44	Type I diabetes mellitus signaling	1.71	CD247, MAP2K6, SOCS3, ICA1, MAPK8, IFNGR2, HLA-DRB1, HLA-DMB, IFNGR1, PRF1, GAD1, FCER1G, HLA-DOB, BID, IL1B, TNFRSF1B, TNFRSF11B, GZMB

Continued

Table II *Continued*

	Ingenuity canonical pathways	−log(*P*-value)	Molecules
45	Atherosclerosis signaling	1.68	IL1A, PLA2G12A, MMP3, CXCR4, CD36, SELPLG, TNFRSF12A, COL1A2, PLA2G4A, TGFB1, LPL, IL1B, PLA2G4F, PDGFD, MMP1, ITGA4
46	Role of NFAT in cardiac hypertrophy	1.61	MAP2K6, LIF, TGFBR1, CAMK1D, RCAN2, HDAC9, CAMK2D, GNG11, PLCE1, TGFB1, TGFB2, MRAS, AKT3, PLCB1, GNG4, PRKD3, PRKCA, GNAS, PRKCQ, HDAC2, MAPK8, MEF2A, RCAN1, PLCB4, PRKAG2, PIK3CD, GNG2
47	Tryptophan metabolism	1.59	ECHS1, ACAT2, CYP3A5, BCKDHB, CYP3A4, CYP2C18, SRD5A3, DHCR24, ALDH3A2, CYP4B1, ACAT1, CYP4X1, CYP2J2, SMOX, EHHADH, HADH, CYP51A1, MAOA
48	Hepatic fibrosis/hepatic stellate cell activation	1.58	IL1A, TGFBR1, FGF2, IFNGR2, IFNGR1, IGFBP5, MMP2, IFNAR2, COL1A2, TGFB1, KDR, IGFBP3, PDGFRA, LAMA1, TGFB2, IL10RA, IL1B, ECE1, TNFRSF1B, MMP1, TNFRSF11B, TIMP2
49	Tyrosine metabolism	1.55	ADH5, ALDH3B2, IYD, DHRS9, DBT, PECR, GOT1, SMOX, HGD, DHRS4, MAOA, BCKDHB
50	Axonal guidance signaling	1.54	RAC2, GLI2, EPHB2, ADAM28, MRAS, PLCB1, PRKD3, FZD2, ITGA4, PRKCQ, RAC3, SRGAP3, MYL12A, ADAM12, FZD6, PIK3CD, GNG2, PDGFD, RAP1B, FZD10, MMP7, RND1, BMP2, ABL1, EPHA4, SEMA4C, WNT7A, GNG11, SDC2, ADAM19, AKT3, RASSF5, ERBB2, GNG4, SEMA3F, PRKCA, GNAS, PLXNC1, NRP2, PAK6, CXCR4, TUBB2C, GNA12, ITGA2, TUBA4A, MMP10, PLCB4, WIPF1, FZD4, SEMA4D, PRKAG2, WNT5A
51	Cholecystokinin/gastrin-mediated signaling	1.53	MAP2K6, IL1A, PRKCQ, GNA12, MAPK8, MEF2A, EPHA4, RHOJ, PLCB4, RHOB, CREM, MRAS, PLCB1, IL1B, SST, PRKD3, PRKCA
52	Germ cell–sertoli cell junction signaling	1.53	MAP2K6, EPN3, PLS1, RAC2, TGFBR1, MAP3K6, PAK6, TUBB2C, ITGA2, MAPK8, TUBA4A, RHOJ, RAC3, CTNNA2, RHOB, TGFB1, MRAS, TGFB2, ZYX, PIK3CD, ACTG2, CTNNB1, RAB8B, PVRL2
53	Fatty acid elongation in mitochondria	1.48	ECHS1, PECR, EHHADH, ACAA2, HADH
54	Glycosphingolipid biosynthesis–ganglioseries	1.48	ST3GAL2, ST8SIA4, GM2A, DBT, ST8SIA2, ST3GAL5
55	TREM1 signaling	1.45	TREM1, NOD2, TLR5, TYROBP, LAT2, AKT3, IL1B, TLR3, CCL3, ITGAX
56	Glycerophospholipid metabolism	1.41	NAPEPLD, DGKD, PLA2G12A, PISD, PLD1, AGPAT4, PLA2G4A, PLCB4, PLCE1, CDS1, PCYT2, PLCB1, DBT, GOT1, PLA2G4F, LPIN2, AGPAT9, PPAP2C
57	Lysine degradation	1.40	AASDH, KAT2B, AASDHPPT, ECHS1, ACAT2, ALDH3A2, ACAT1, DBT, SHMT1, EHHADH, HADH
58	NF-κB signaling	1.39	MAP2K6, IL1A, TGFBR1, PRKCQ, HDAC2, RELB, BMP2, MAPK8, BMPR2, MAP4K4, TNIP1, TLR5, CARD10, KDR, PDGFRA, MRAS, FCER1G, AKT3, IL1B, PIK3CD, TRAF5, TLR3, TNFRSF1B, TNFRSF11B
59	Airway pathology in chronic obstructive pulmonary disease	1.37	MMP8, MMP2, MMP1
60	Ovarian cancer signaling	1.37	CDKN2A, FZD10, MMP7, TCF4, PTGS1, ABL1, MMP2, TCF3, TCF7, FZD4, WNT7A, MRAS, FZD6, PRKAG2, AKT3, PIK3CD, BRCA1, CTNNB1, FZD2, WNT5A
61	Glioblastoma multiforme signaling	1.36	CDKN2A, FZD10, CDK6, RHOJ, TCF3, CCNE1, PLCB4, FZD4, PLCE1, WNT7A, RHOB, TSC2, PDGFRA, MRAS, FZD6, PLCB1, AKT3, PIK3CD, PDGFD, CTNNB1, FZD2, WNT5A
62	PXR/RXR activation	1.31	CPT1A, PCK2, CYP3A4, ALDH3A2, PRKAG2, AKT3, IGFBP1, ABCC3, NR3C1, CYP3A5, ABCB9

In total, 62 pathways were found to be involved. The associated molecules found in the mentioned pathways are shown.

(Bonduelle *et al.*, 1988). However, due to the absence of direct vascular communication, the secretion of hCG into the maternal circulation is initially limited (Nepomnaschy *et al.*, 2008), indicating that in hCG-triggered ovarian stimulation cycles, the actions of LH during the early luteal phase is covered by the triggering bolus of hCG and after this period, by the hCG gradually produced by the implanting embryo. However, after GnRH agonist triggering, the combined effect of ovarian stimulation and GnRH agonist triggering reduces the endogenous LH level dramatically (Humaidan, 2009) and, although a standard luteal phase support is used, the reduction in LH will have a detrimental effect on the reproductive outcome (Humaidan *et al.*, 2005; Kolibianakis *et al.*, 2005).

In the present study, the control group (A) represented the standard GnRH antagonist protocol in which final oocyte maturation was performed with a bolus of 10 000 IU hCG, followed by a standard luteal phase support. Group B represented a standard GnRH

Table III From this data set, 25 networks could be formed in Ingenuity.

	Molecules in network	Top functions
1	ADK, ANKLE2, ASPN, C21orf33, CRMP, CRMP1, DPYSL3, DPYSL4, DYRK2, FILIP1L, FNDC3B, HOXB5, KDM6B, KIF3C, LANCL1, LOXL2, LPCAT3, LRBA, LRRC1, MFAP2, MRPS6, PI4K2B, PKIG, PLXNC1, RAB25, RAMP2, RBMS1, SLC39A8, SLC39A14, SMOC2, ST3GAL5, TAX1BP3, TGFB1, UCK2, ZFP36L2	Cell morphology, skeletal and muscular system development and function, molecular transport
2	ADIPOR2, ALAD, ATG7, ATG16L1, BCAT2, BCKDHB, CLEC3B, CMAS, EHHADH, ERBB2, GDPD3, GIPC2, HTATIP2, LXN, MAN1A1, MAN1A2, MAN2B2, Mannosidase Alpha, MAP1B, MAPK8, MCCC1, MDFIC, MTR, NPTX2, OASL, PBX3, POLB, PRR15L, PTN, RNA polymerase II, SEMA4C, SH2D1B, TARBP1, TFIIH, TSC22D1	Cellular response to therapeutics, amino acid metabolism, small molecule biochemistry
3	B3GNT5, BCL11A, CARD10, CBR3, CORO1A, CRIP1, CRISP3, DBT, EDA, EHF, EOMES, EZH1, FAIM, FAM46A, HTRA1, IL13RA2, KLF3, LITAF, lymphotoxin-alpha1-beta2, MTF2, NFkB (complex), NMRAL1, OFD1, peptidase, PNKD, SLC15A2, TEAD2, TNFRSF18, TNFRSF10B, TNFRSF10D, Trail-R, UNC5CL, VGLL1, VOPP1, ZFAND5	Molecular transport, organismal development, skeletal and muscular system development and function
4	AQP3, BCAT1, BRP44L, C11orf9, C14orf147, CEP170, Cg, CXorf40A/CXorf40B, DHCR24, DHRS3, DPY19L1, ECE1, EFEMP1, EMB, FJX1, FSH, GEM, GNLY, GRK5, hCG, KDM5B, LGALS3BP, Lh, LSS, MT1H, MT1X, MT2A, PMAIP1, POP5, PPARGC1B, PSD3, RNASET2, SC4MOL, TMED4, TMEM14A	Cell morphology, cancer, reproductive system disease
5	ALCAM, ATPIF1, CNKSR2, CNKSR3, DLGAP1, DLGAP4, DUSP2, ERK1/2, HABP2, IL17RD, KCND2, KLRC1, KLRC3, KLRD1, KLRK1, LAT2, MAGI, MAGI2, MAGI3, NRCAM, NRP2, PALLD, PDCD2, PDGF-AA, Potassium Channel, PPAP2C, SEMA3F, SH3GLB2, SMAD1/5, SORBS2, TMEM22, TREM1, TRIB1, TYROBP, VANGL2	Cellular movement, nervous system development and function, cell-to-cell signaling and interaction
6	AKT3, Beta Arrestin, C3AR1, CD97, FPR3, FZD2, FZD4, FZD6, FZD10, Gpcr, GPR18, GPR37, GPR65, GPR97, GPR110, GPR115, GPR157, GPR160, GPR171, GPR183, GPR137B, GPRC5B, HTR2B, LGR4, LGR5, LPAR2, LPAR3, Metalloprotease, OPRK1, RAC2, Relaxin, RGS1, RXFP1, S1PR2, Sfk	Cell signaling, auditory disease, neurological disease
7	Akt, ANGPTL1, Ant, ASAH1, AZGP1, Calcineurin A, CDC14B, Ceramidase, Collagen Alpha1, CREG1, FBXO32, FKBP4, FKBP5, FOXC1, HDGFRP3, HPGD, IKBIP, KIR2DL4/LOC100287534, NAAA, NEBL, peptidylprolyl isomerase, PPID, PRKAG2, SEC14L2, SLC25A4, SMURF2, TCN1, THBS2, THEM4, TIE1, TNFAIP6, TPD52, TPD52L1, WFDC2, YPEL1	Cellular assembly and organization, endocrine system development and function, lipid metabolism
8	ACAT2, ARHGEF2, ATP2A3, Cbp/p300, COL1A2, EGR1, ETS1, FAM171A1, FGF2, FLI1, GABRE, GNG2, HOXB7, Hsp27, IER3, IL1A, INHBA, JUNB, KIAA1712, MAP2K6, MBIP, NFkB (family), NfkB1-RelA, NINL, P4HA1, PTBP2, Ras homolog, RELB, RHOB, Sox, SOX4, SOX9, SOX17, VDR, ZNF250	Cellular growth and proliferation, gene expression, cellular development
9	Alpha Actinin, Alpha catenin, ANK3, Cadherin, CAMK2N1, CDH11, CDH16, CHL1, CHST4, CSRP2, CTH, CTNNA2, CXCL13, EBP, EBPL, EDN3, ERK, Fcer1, GNA12, GSR, IFN ALPHA RECEPTOR, IFRD1, IL10RA, LAMA1, Laminin1, MT1F, PJA1, PTPRC, PTPRE, PTPRM, PVRL2, SEMA4D, SPSB1, SPTBN1, TCF7	Cell morphology, cellular development, cardiovascular system development and function
10	ADAM28, AMD1, c-Src, C5orf13, Calpain, CD36, Collagen type I, CPT1A, FGR, FHL2, Integrin, ITGA2, ITGB3, JAM2, KDR, MMP14, NME3, NRBP2, NUAK1, PDGF BB, PDGFRA, Plasminogen Activator, PLAU, SCARB1, SELPLG, SERPINA5, SLC6A6, SLC7A7, SNX20, SRC, TFPI, TGFB2, TGM2, THBS1, TPST1	Cell-to-cell signaling and interaction, cellular function and maintenance, inflammatory response
11	AGPAT9, ARNT2, BAG2, BST1, CCR1, COL12A1, CRISP2, CSNK1E, DUB, DUOX1, EML2, EMP1, GALNT4, GALNT12, Gelatinase, Glutathione peroxidase, GPX2, LTBP2, MARCKS, MT1G, MUC1, MUC7, Mucin, NDRG2, NEK6, p70 S6k, PMEPA1, PRKCQ, PROM1, RAD54B, SNN, Tgf beta, USP9X, Vegf, ZDHHC14	Lipid metabolism, small molecule biochemistry, cancer
12	ABHD5, Actin, AEBP1, ATP6V0E2, ATP6V1C2, ATP6V1G1, ATP6V1H, ATP8A2, ATPase, CBLC, ENC1, EPS8L1, ETV5, GCNT1, H+-transporting two-sector ATPase, JUB, LEFTY2, Mapk, MLPH, MYRIP, PCSK5, PLAGL1, PLIN2, PLIN3, PLS1, Rab5, RAB27B, RABGEF1, Rho gdi, RHOBTB3, SORD, SYTL4, Tni, Vacuolar H+ ATPase, WISP1	Cellular assembly and organization, hair and skin development and function, lipid metabolism
13	ANKRD5, ARHGAP9, Arp2/3, AXL, CTTN, CYFIP2, FCGR1A/2A/3A, Fgf, Fgfr, FOXQ1, FRMD6, Hspg, KAL1, LRRC41, Pak, PAK6, Par6, PARD6G, PDLIM4, PIP5K1B, PLXDC1, PNMA1, Rac, RAC3, RAI14, RASSF8, RBFOX2, RBPMS, SDC2, SRGAP3, SSBP3, STRBP, TIAM2, TLE6, ZNF226	Cellular assembly and organization, nervous system development and function, connective tissue development and function

Continued

Table III *Continued*

	Molecules in network	Top functions
14	AHCYL2, ANKS1A, ATF3, DHRS1, ERBB4, Estrogen Receptor, FAM89B, FOLR1, GC-GCR dimer, HMGA1, HSD11B2, ID1, ID3, IL2RB, IP6K2, JAZF1, NFIA, NFIB, NPDC1, Nuclear factor 1, p85 (pik3r), PCK2, PEPCK, PHB, PLSCR1, PPARG, SGIP1, Shc, SMARCA2, SPECC1, SWI-SNF, TBXAS1, Thymidine Kinase, TYSND1, XDH	Gene expression, cellular growth and proliferation, tumor morphology
15	ACAT1, Alp, Ap1, ATAD2, BLVRA, CHIC2, Creb, CSRNP2, DAXX, DBC1, DEAF1, DPP7, EPB41L4B, GAS1, HGD, Histone h3, Histone h4, HOXB8, IL1, MEST, MOAP1, MTL5, NR3C1, PHC1, POU2F3, PRKAC, PRRC2C, PTCD2, RPS6KA3, Rsk, RUNX2, SCNN1A, SVIL, TNFRSF1B, TP53I3	Connective tissue disorders, developmental disorder, skeletal and muscular disorders
16	3',5'-cyclic-GMP phosphodiesterase, 3',5'-cyclic-nucleotide phosphodiesterase, ABHD3, ACAA2, ADCY, AHNAK, ATP2B2, BICD1, Calmodulin, CaMKII, CYP24A1, Cytoplasmic Dynein, DYNC1I1, EEF2K, G protein alpha, GAD1, GAL, GPCPD1, Gs-coupled receptor, HIC1, KCTD10, LIF, LRP8, MYO1B, NCAM1, PDE10A, PDE4B, PDE6A, PDE9A, SFXN3, ST8SIA4, SYNJ2, SYNJ2BP, WNT5A, ZG16B	Nucleic acid metabolism, small molecule biochemistry, cell signaling
17	ARHGAP20, CAPN6, CYBA, EXOC4, FHIT, G protein beta gamma, GCHFR, GNAS, GNG4, GNG11, KSR1, LRRFIP1, MRAS, NADPH oxidase, PDCL, phosphoinositide phospholipase C, Pka, Plc beta, PLCB1, PLCB4, PLCE1, RAB31, RALA, Rap, Rap1, RAP1B, RAP2B, RASSF5, SEPT4, SEPT6, Septin, SLC9A3R1, SORL1, TSC2, TSH	Cancer, reproductive system disease, cell morphology
18	26s Proteasome, ABL1, ARRDC1, ARRDC2, BACH1, C1QTNF5, CBX3, CCDC50, CREM, DIO2, DLAT, DNMT3A, EGR2, Gm-csf, Hsp70, Hsp90, KIFC2, LRP, LRP4, P38 MAPK, PDK4, PIM1, PRSS23, RNF125, RNF150, SHMT1, SLC39A4, SOCS3, Sod, ST5, STAT5a/b, TNIP1, TNNC1, UBE2D4, Ubiquitin	Cell morphology, infection mechanism, lipid metabolism
19	ACP5, ACSL, ACSL3, ACSL4, ADAM19, Adaptor protein 1, AMT, AP1S3, Ctbp, CUX1, EVI2A, FAM65B, GCSH, GLRX, Hat, HDAC2, HIST1H4C (includes others), HISTONE, IKZF1, KAT2B, KLF15, LOC100505603/PNRC2, LPIN2, Mi2, NCOR2, NR4A2, Pias, RBBP4, SATB1, SESN3, Sin3A, SLC27A2, STAT, TBX3, ZBTB16	Genetic disorder, metabolic disease, lipid metabolism
20	CD247, CYGB, EMG1, Fcgr3, Gα12/13, HAVCR2, HCLS1, ITK, KHDRBS1, LCP2, Lpa receptor, MTCH2, NFAT (complex), PACSIN2, PAG1, PI3K (complex), PIK3AP1, PLC gamma, PLEKHO1, PODXL, RAB4A, SAMSN1, SBK1, SH2D2A, SLA, SLA2, SLC25A38, SMPDL3B, SYK/ZAP, TAF1A, TEC/BTK/ITK/TXK/BMX, VAV, Vegf Receptor, WIPF1, YTHDC1	Cell signaling, molecular transport, vitamin and mineral metabolism
21	ABCB9, CHST11, CHST15, CTNNβ-TCF/LEF, CYB5A, CYP2C18, CYP2J2, CYP3A4, CYP3A5, CYP4B1, CYP4X1, CYP51A1, DCXR, glutathione transferase, GST, GSTK1, GSTO1, HS3ST1, HS3ST3A1, HS6ST1, HS6ST3, Ikb, IKK (complex), MGST1, MGST2, Ncoa-Nr1i2-Rxra, PXR ligand-PXR-Retinoic acid-RXRα, sulfotransferase, SULT1C2, SULT1E1, TMCO1, Tnf receptor, TNFRSF11B, unspecific monooxygenase, VEPH1	Small molecule biochemistry, endocrine system development and function, drug metabolism
22	ACSS2, B3GALT5, CLDN1, CLDN10, COL4A2, DIO3, ECI2, EIF4EBP2, ERCC5, ERRFI1, GHRHR, GRB10, ISLR, LEFTY2, MAGED4/MAGED4B, MAP2, MAPK6, MARCKS, MERTK, MIA, MIOS, mir-214, NOV, NTHL1, PLCE1, PPP1R16B, RAE1, SLA, SLC27A2, SLC5A3, SLFN5, SRD5A3, TLR5, tretinoin, ZNF600/ZNF888	Tissue morphology, cell death, cellular function and maintenance
23	ACVR1, BMP, BMP2, BMPR2, CDK14, EPHA4, EPHB2, EVC2, FBLIM1, FGD6, Filamin, G-protein beta, Gi-coupled receptor, GRB10, GREM1, HIST2H2BE (includes others), MAP4K4, MEGF10, NBL1, NCK, NOG, Notch, NPR3, RHOBTB1, RHOJ, Sapk, Secretase gamma, SLC26A2, Smad, SMAD9, Smad1/5/8, SMURF1, TGFBR, TGFBR1, TRAF5	Cellular development, connective tissue development and function, skeletal and muscular system development and function
24	ARL4D, BCL2A1, BCR, BLVRB, Cbp, CXADR, Fc gamma receptor, GMPR, HES1, HIPK2, Iga, IgG1, IgG2a, Igm, Immunoglobulin, ITGAM, KIR, MHC CLASS I (family), MITF, MPHOSPH6, PRDM1, Ptk, PTK7, RUNX1, SASH3, SIRPA, SIX4, SLC22A4, SMOX, TCF4, TCF3/4, TLE1, TLE2, TLE3, TRIM2	Cellular development, gene expression, cell-to-cell signaling and interaction
25	ABCC3, ANXA9, Bcl9-Cbp/p300-Ctnnb1-Lef/Tcf, CEP70, CERK, Coup-Tf, CPB2, CYP19, CYP26A1, DUSP5, Esr1-Esr1-estrogen-estrogen, GM2A, HPRT1, IER2, Igh, IL1B, JINK1/2, KLF10, LGALS9, MMD, N-cor, NLRP1, NOD2, NRIP1, PANX1, PCDH7, Rar, RCAN2, Retinoic acid-RAR-RXR, Rxr, SLC20A1, SLC2A9, T3-TR-RXR, Thyroid hormone receptor, UAP1	Cell signaling, drug metabolism, genetic disorder

The functions associated with the found networks are shown.

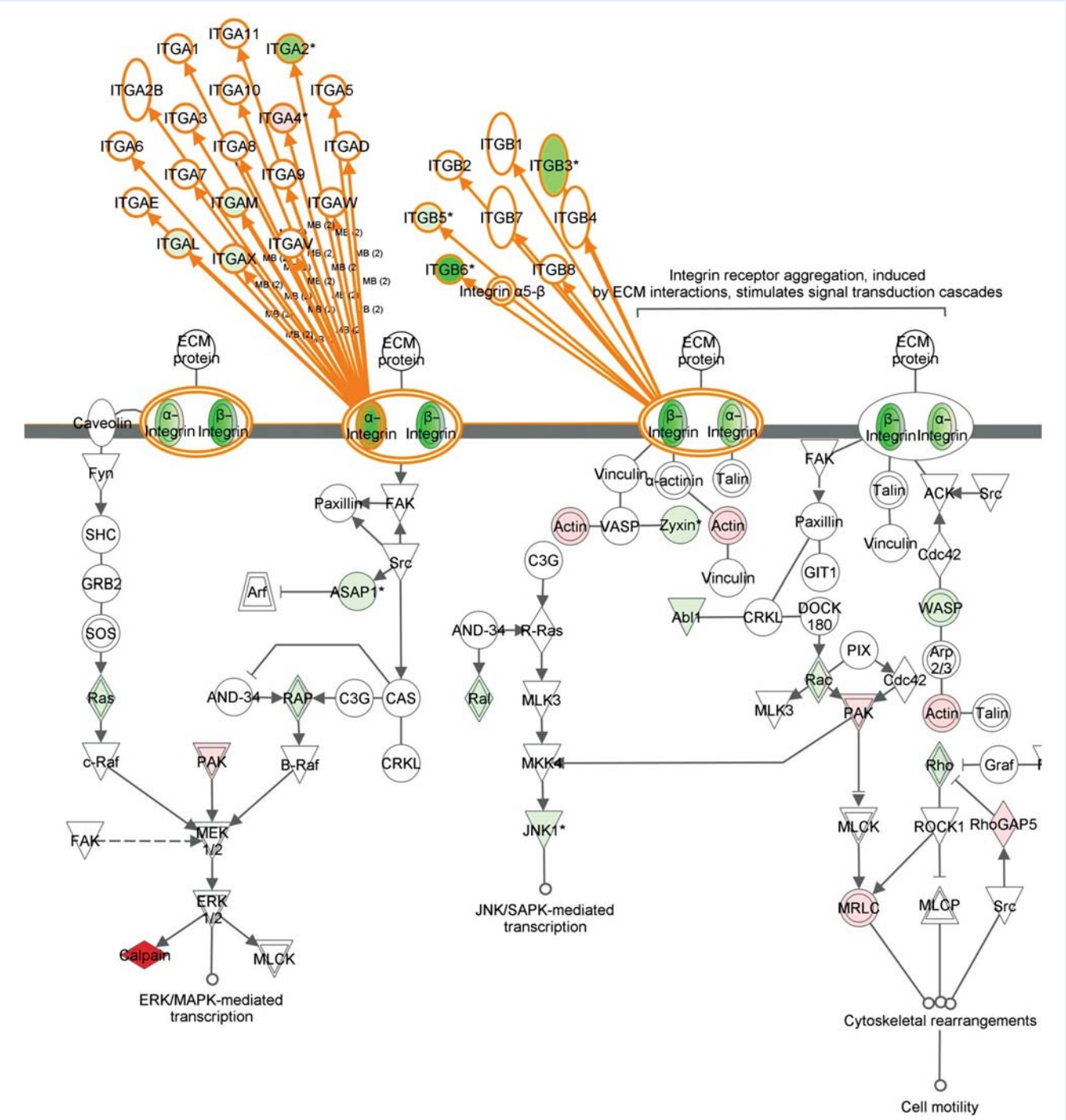

Figure 2 Part of the integrin signaling pathway, from which we validated ITGB6.

antagonist protocol with the GnRH agonist trigger, followed by a modified luteal phase support, consisting of a bolus of 1500 IU hCG administered on the day of oocyte retrieval along with the standard luteal phase support. This concept has recently been shown to secure the ongoing clinical pregnancy rate after the GnRH agonist trigger (Humaidan *et al.*, 2006, 2010). Group C represented the GnRH agonist trigger, followed by a standard luteal phase support only. This concept previously resulted in an extremely low clinical ongoing pregnancy rate and a high early pregnancy loss rate (Humaidan *et al.*, 2005; Kolibianakis *et al.*, 2005). Finally, Group D received the GnRH agonist trigger and no luteal phase support, mimicking the conditions of the study by Beckers *et al.* (2003), also reporting low clinical ongoing pregnancy rates.

When comparing the microarray analysis between groups, significant differences were seen in gene expression between Group A or B and Group C or D, whereas only a slight difference was seen

between Groups A and B, supporting the clinical finding of a normalization of the luteal phase after the GnRH agonist trigger if the patient is supplemented with a bolus of 1500 IU hCG (Humaidan et al., 2006, 2010). In the validation of several genes with a more quantitative technique such as RT–PCR, we found a large standard deviation between the samples of the same groups. Therefore, some individual genes did not reach significance in the real-time RT–PCR. This large variation is possibly due to an inter-individual variation between patients.

Most of the genes with extreme up- or down-regulation in Group D (Fig. 1) and the genes found to be significantly differentially regulated between Groups B and C are well-known for their roles during implantation (Tabibzadeh, 2002; Macklon et al., 2008; Van Vaerenbergh et al., 2011). Other genes found to be highly up-regulated in the microarray data are MMPs, integrins and interleukins. MMPs are involved in a number of pathways, like the leukocyte extravasation signaling pathway. Moreover, it is known from the literature (Pilka et al., 2003) that MMPs play a role in extracellular matrix degradation and MMP26 is expressed in a cyclic pattern in the human endometrium. Its expression is increased from the proliferative to the early secretory phase. Therefore, MMP26 may play a role in implantation either directly or as an activator of cytokines, growth factors and other vasoactive factors. ITGB6 is one of the integrins expressed in the integrin signaling pathway (Fig. 2). Integrins are well known cell adhesion molecules present in the endometrium throughout the menstrual cycle, established as potential markers of endometrial receptivity and known participants in embryo-endometrial interactions (Lindhard et al., 2002). Interleukins are known fertility-related factors as well (Ledee-Bataille et al., 2004, 2005). These findings demonstrate that known fertility-related genes are differently regulated during the window of implantation when the mode of triggering is modified and when there is no luteal phase support.

Taken together, a bolus of GnRH agonist (triptorelin, 0.2 mg) is sufficient to secure final oocyte maturation, but this triggering concept further disrupts the luteal phase insufficiency commonly seen in all ovarian stimulation cycles, with or without a standard luteal phase support (Groups C and D). However, the combination of the GnRH agonist trigger and a modified luteal phase support (Group B) shifts the endometrial gene expression pattern toward the pattern seen after the hCG trigger (Group A).

In conclusion, the gene expression of endometrial biopsies taken on Day 5 after oocyte retrieval from oocyte donors, using different protocols for final oocyte maturation and luteal phase support, showed significant differences between groups. Many genes involved are known to play a role in implantation and the receptivity of the endometrium. Whether the differences in gene expression are directly associated with an increase in LH activity levels, an increase in progesterone levels or both, needs to be further elucidated. The lessons learned from the GnRH agonist trigger may pave the way for a wider understanding of the luteal physiology of the stimulated cycle. This could potentially lead to future changes in the luteal phase support which might increase the numbers of embryos implanting after IVF.

Supplementary data

Supplementary data are available at http://humrep.oxfordjournals.org/.

Acknowledgements

The authors wish to thank the doctors, nurses and lab technicians from Centre for Reproductive Medicine, Dutch-speaking Free University of Brussels, Belgium, and Unit of Reproductive Immunology and Implantation, Dutch-speaking Free University of Brussels Belgium for their excellent help during this study.

Authors' roles

All the authors contributed substantially to the analysis and interpretation of data, writing of manuscript and approval of the final version. P.H. specially contributed to the planning and design of study. I.V.V. contributed to RNA isolation, microarray data analysis and QPCR data analysis. C.Bo. contributed to endometrial sample evaluation and interpretation of gene array data. C.Bl. contributed in the recruitment of patients. F.S. and L.L. contributed to microarray data acquisition.

Funding

This study was supported by an unrestricted grant from MSD, Belgium.

Conflict of interest

None declared.

References

Andersen CY, Humaidan P, Ejdrup HB, Bungum L, Grondahl ML, Westergaard LG. Hormonal characteristics of follicular fluid from women receiving either GnRH agonist or hCG for ovulation induction. *Hum Reprod* 2006;**21**:2126–2130.

Beckers NG, Macklon NS, Eijkemans MJ, Ludwig M, Felberbaum RE, Diedrich K, Bustion S, Loumaye E, Fauser BC. Nonsupplemented luteal phase characteristics after the administration of recombinant human chorionic gonadotropin, recombinant luteinizing hormone, or gonadotropin-releasing hormone (GnRH) agonist to induce final oocyte maturation in in vitro fertilization patients after ovarian stimulation with recombinant follicle-stimulating hormone and GnRH antagonist cotreatment. *J Clin Endocrinol Metab* 2003;**88**:4186–4192.

Bonduelle ML, Dodd R, Liebaers I, Van Steirteghem A, Williamson R, Akhurst R. Chorionic gonadotrophin-beta mRNA, a trophoblast marker, is expressed in human 8-cell embryos derived from tripronucleate zygotes. *Hum Reprod* 1988;**3**:909–914.

Damewood MD, Shen W, Zacur HA, Schlaff WD, Rock JA, Wallach EE. Disappearance of exogenously administered human chorionic gonadotropin. *Fertil Steril* 1989;**52**:398–400.

Duffy DM, Stewart DR, Stouffer RL. Titrating luteinizing hormone replacement to sustain the structure and function of the corpus luteum after gonadotropin-releasing hormone antagonist treatment in rhesus monkeys. *J Clin Endocrinol Metab* 1999;**84**:342–349.

Edwards RG, Fishel SB, Cohen J, Fehilly CB, Purdy JM, Slater JM, Steptoe PC, Webster JM. Factors influencing the success of in vitro fertilization for alleviating human infertility. *J In Vitro Fert Embryo Transf* 1984;**1**:3–23.

Engmann L, DiLuigi A, Schmidt D, Nulsen J, Maier D, Benadiva C. The use of gonadotropin-releasing hormone (GnRH) agonist to induce oocyte

maturation after cotreatment with GnRH antagonist in high-risk patients undergoing in vitro fertilization prevents the risk of ovarian hyperstimulation syndrome: a prospective randomised controlled study. *Fertil Steril* 2008;**89**:84–91.

Eppig JJ. FSH stimulates hyaluronic acid synthesis by oocyte-cumulus cell complexes from mouse preovulatory follicles. *Nature* 1979; **281**:483–484.

Fatemi HM, Popovic-Todorovic B, Donoso P, Papanikolaou E, Smitz J, Devroey P. Luteal phase oestradiol suppression by letrozole: a pilot study in oocyte donors. *Reprod Biomed Online* 2008;**17**:307–311.

Fauser BC, de Jong D, Olivennes F, Wramsby H, Tay C, Itskovitz-Eldor J, van Hooren HG. Endocrine profiles after triggering of final oocyte maturation with GnRH agonist after cotreatment with the GnRH antagonist ganirelix during ovarian hyperstimulation for in vitro fertilization. *J Clin Endocrinol Metab* 2002;**87**:709–715.

Gonen Y, Balakier H, Powell W, Casper RF. Use of gonadotropin-releasing hormone agonist to trigger follicular maturation for in vitro fertilization. *J Clin Endocrinol Metab* 1990;**71**:918–922.

Griesinger G, Kolibianakis EM, Papanikolaou EG, Diedrich K, Van Steirteghem A, Devroey P, Ejdrup BH, Humaidan P. Triggering of final oocyte maturation with gonadotropin-releasing hormone agonist or human chorionic gonadotropin. Live birth after frozen-thawed embryo replacement cycles. *Fertil Steril* 2007;**88**:616–621.

Hoff JD, Quigley ME, Yen SS. Hormonal dynamics at midcycle: a reevaluation. *J Clin Endocrinol Metab* 1983;**57**:792–796.

Humaidan P. Luteal phase rescue in high-risk OHSS patients by GnRHa triggering in combination with low-dose HCG: a pilot study. *Reprod Biomed Online* 2009;**18**:630–634.

Humaidan P, Bredkjaer HE, Bungum L, Bungum M, Grondahl ML, Westergaard L, Andersen CY. GnRH agonist (buserelin) or hCG for ovulation induction in GnRH antagonist IVF/ICSI cycles: a prospective randomized study. *Hum Reprod* 2005;**20**:1213–1220.

Humaidan P, Bungum L, Bungum M, Yding AC. Rescue of corpus luteum function with peri-ovulatory HCG supplementation in IVF/ICSI GnRH antagonist cycles in which ovulation was triggered with a GnRH agonist: a pilot study. *Reprod Biomed Online* 2006;**13**:173–178.

Humaidan P, Ejdrup BH, Westergaard LG, Yding AC. 1500 IU human chorionic gonadotropin administered at oocyte retrieval rescues the luteal phase when gonadotropin-releasing hormone agonist is used for ovulation induction: a prospective, randomized, controlled study. *Fertil Steril* 2010;**93**:847–854.

Humaidan P, Westergaard LG, Mikkelsen AL, Fukuda M, Yding AC. Levels of the epidermal growth factor-like peptide amphiregulin in follicular fluid reflect the mode of triggering ovulation: a comparison between gonadotrophin-releasing hormone agonist and urinary human chorionic gonadotrophin. *Fertil Steril* 2011;**95**:2034–2038.

Imoedemhe DA, Sigue AB, Pacpaco EL, Olazo AB. Stimulation of endogenous surge of luteinizing hormone with gonadotropin-releasing hormone analog after ovarian stimulation for in vitro fertilization. *Fertil Steril* 1991;**55**:328–332.

Itskovitz J, Boldes R, Levron J, Erlik Y, Kahana L, Brandes JM. Induction of preovulatory luteinizing hormone surge and prevention of ovarian hyperstimulation syndrome by gonadotropin-releasing hormone agonist. *Fertil Steril* 1991;**56**:213–220.

Kessler MJ, Reddy MS, Shah RH, Bahl OP. Structures of N-glycosidic carbohydrate units of human chorionic gonadotropin. *J Biol Chem* 1979;**254**:7901–7908.

Kolibianakis EM, Tarlatzis B, Devroey P. GnRH antagonists in IVF. *Reprod Biomed Online* 2005;**10**:705–712.

Ledee-Bataille N, Olivennes F, Kadoch J, Dubanchet S, Frydman N, Chaouat G, Frydman R. Detectable levels of interleukin-18 in uterine luminal secretions at oocyte retrieval predict failure of the embryo transfer. *Hum Reprod* 2004;**19**:1968–1973.

Ledee-Bataille N, Bonnet-Chea K, Hosny G, Dubanchet S, Frydman R, Chaouat G. Role of the endometrial tripod interleukin-18, -15, and -12 in inadequate uterine receptivity in patients with a history of repeated in vitro fertilization-embryo transfer failure. *Fertil Steril* 2005; **83**:598–605.

Lindhard A, Bentin-Ley U, Ravn V, Islin H, Hviid T, Rex S, Bangsboll S, Sorensen S. Biochemical evaluation of endometrial function at the time of implantation. *Fertil Steril* 2002;**78**:221–233.

Macklon NS, van der Gaast MH, Hamilton A, Fauser BC, Giudice LC. The impact of ovarian stimulation with recombinant FSH in combination with GnRH antagonist on the endometrial transcriptome in the window of implantation. *Reprod Sci* 2008;**15**:357–365.

Mannaerts BM, Geurts TB, Odink J. A randomized three-way cross-over study in healthy pituitary-suppressed women to compare the bioavailability of human chorionic gonadotrophin (Pregnyl) after intramuscular and subcutaneous administration. *Hum Reprod* 1998; **13**:1461–1464.

Nepomnaschy PA, Weinberg CR, Wilcox AJ, Baird DD. Urinary hCG patterns during the week following implantation. *Hum Reprod* 2008; **23**:271–277.

Oktay K, Turkcuoglu I, Rodriguez-Wallberg KA. GnRH agonist trigger for women with breast cancer undergoing fertility preservation by aromatase inhibitor/FSH stimulation. *Reprod Biomed Online* 2010; **20**:783–788.

Pilka R, Whatling C, Domanski H, Hansson S, Eriksson P, Casslen B. Epithelial expression of matrix metalloproteinase-26 is elevated at mid-cycle in the human endometrium. *Mol Hum Reprod* 2003; **9**:271–277.

Porter RN, Smith W, Craft IL, Abdulwahid NA, Jacobs HS. Induction of ovulation for in-vitro fertilisation using buserelin and gonadotropins. *Lancet* 1984;**2**:1284–1285.

Rosenberg SM, Luciano AA, Riddick DH. The luteal phase defect: the relative frequency of, and encouraging response to, treatment with vaginal progesterone. *Fertil Steril* 1980;**34**:17–20.

Strickland S, Beers WH. Studies on the role of plasminogen activator in ovulation. In vitro response of granulosa cells to gonadotropins, cyclic nucleotides, and prostaglandins. *J Biol Chem* 1976; **251**:5694–5702.

Tabibzadeh S. Homeostasis of extracellular matrix by TGF-beta and lefty. *Front Biosci* 2002;**7**:d1231–d1246.

Tavaniotou A, Devroey P. Luteal hormonal profile of oocyte donors stimulated with a GnRH antagonist compared with natural cycles. *Reprod Biomed Online* 2006;**13**:326–330.

Tavaniotou A, Albano C, Smitz J, Devroey P. Comparison of LH concentrations in the early and mid-luteal phase in IVF cycles after treatment with HMG alone or in association with the GnRH antagonist *Cetrorelix*. *Hum Reprod* 2001;**16**:663–667.

Van Lommel L, Janssens K, Quintens R, Tsukamoto K, Vander MD, Lemaire K, Denef C, Jonas JC, Martens G, Pipeleers D *et al.* Probe-independent and direct quantification of insulin mRNA and growth hormone mRNA in enriched cell preparations. *Diabetes* 2006; **55**:3214–3220.

Van Vaerenbergh I, Van Lommel L, Ghislain V, In't Veld P, Schuit F, Fatemi HM, Devroey P, Bourgain C. In GnRH antagonist/rec-FSH stimulated cycles, advanced endometrial maturation on the day of oocyte retrieval correlates with altered gene expression. *Hum Reprod* 2009;**24**:1085–1091.

Van Vaerenbergh I, Blockeel C, Van Lommel L, Ghislain V, In't Veld P, Schuit F, Fatemi HM, Devroey P, Bourgain C. Cyclooxygenase-2

network as predictive molecular marker for clinical pregnancy in in vitro fertilization. *Fertil Steril* 2011;**95**:448–51, 451.

Weissman A, Loumaye E, Shoham Z. Recovery of corpus luteum function after prolonged deprivation from gonadotrophin stimulation. *Hum Reprod* 1996;**11**:943–949.

Yding AC. Effect of FSH and its different isoforms on maturation of oocytes from pre-ovulatory follicles. *Reprod Biomed Online* 2002; **5**:232–239.

Yding AC, Leonardsen L, Ulloa-Aguirre A, Barrios-De-Tomasi J, Moore L, Byskov AG. FSH-induced resumption of meiosis in mouse oocytes: effect of different isoforms. *Mol Hum Reprod* 1999;**5**: 726–731.

Zelinski-Wooten MB, Hutchison JS, Hess DL, Wolf DP, Stouffer RL. Follicle stimulating hormone alone supports follicle growth and oocyte development in gonadotrophin-releasing hormone antagonist-treated monkeys. *Hum Reprod* 1995;**10**:1658–1666.